

# A Biomechanical Approach to Investigate the Applicability of the Lake-Thomas Theory in Porcine Aorta

Kenzo Yamamoto<sup>1</sup>, Kazuaki Hara<sup>1</sup>, Hayato Laurence Mizuno<sup>1</sup>, Kosuke Ishikawa<sup>1</sup>, Etsuko Kobayashi<sup>1</sup>, Yuki Akagi<sup>2\*</sup>, Ichiro Sakuma<sup>1</sup>

<sup>1</sup>Graduate School of Engineering,  
The University of Tokyo, Hongo 7-3-1 Bunkyo-ku, Tokyo, 113-8654, JAPAN

<sup>2</sup>Graduate School of Engineering,  
Tokyo University of Agriculture and Technology, Harumichou 3-8-1 Fuchu-shi, Tokyo, 183-8538, JAPAN

\*Corresponding Author

DOI: <https://doi.org/10.30880/ijie.2021.13.05.010>

Received 20 April 2021; Accepted 2 May 2021; Available online 31 July 2021

**Abstract:** Robot-assisted surgeries are procedures where a physician performs surgical maneuvers by operating a robot. One of the main limitations is the difficulty in transferring the surgeon's multiple skills onto the robotic system. Such skills include the ability to estimate the maximum applicable force before damaging the tissue. To implement this skill onto a robotic system, a mathematical model for tissue damage must be developed. The objective of this study is to measure the fracture characteristic in porcine aorta, to then investigate whether an existing fracture model can be applied onto biological tissues. Due to the similarity in the mechanical response between biological tissues and polymeric materials, the model chosen for this study was the Lake-Thomas model. This is the first paper with the aim of validating this model with biological tissues. Two main findings are reported in this investigation. We found that porcine thoracic aorta tears in a specific way which is directly correlated to the tensile direction. The second finding is that an anisotropic linear relationship exists between the critical tearing energy and the elastic modulus, and the elastic modulus to the  $-0.5^{\text{th}}$  power. These results are discussed based on the elastin and collagen fibers, as well as established mathematical equations describing polymer mechanics.

**Keywords:** Biomechanics, collagen, elastin, biological tissue damage, Lake-Thomas model, robot-assisted surgery

## 1. Introduction

When conducting a surgical procedure, the patient undergoes a significant amount of physical stress, such as pain and limited range-of-motion. The patient thus needs time to recover post-surgery. With the increasing collaboration between engineering and medicine, the implementation of robots during surgical procedures as a minimally invasive approach is not uncommon. Robot-assisted surgical technologies such as the *da Vinci Surgical System* are operated by a surgeon to perform surgical procedures. Robot-assisted surgery has multiple advantages, such as an increase in the movement accuracy and overall procedure quality. However, one of its major limitations is the difficulty in transferring the surgeon (operator)'s surgical skill onto the robotic system [1].

During conventional surgery, surgeons rely on their senses to adapt their movements during tissue handling. This is done in order not to apply a load that is greater than what the tissue can handle. This tissue handling skill can be broken down into three main steps. The first step consists of the surgeon observing the biological tissue's deformation response when a specific load is being applied onto it. In the second step, the surgeon estimates the maximum force that can be applied onto the tissue without causing any damage onto it. In this step, the surgeon first estimates the overall mechanical property of the handled tissue based on the observed tissue-tool interaction from the first step. The surgeon

then gauges a safety range in the application force from the tissue’s overall mechanical property, such as its elastic modulus. In the third step, the surgeon adjusts the application force based on the threshold estimated in the previous step. The tissue handling skill is a critical skill during surgery, because damaging a biological tissue, such as a blood vessel, can result in a vital mistake. Multiple studies have been conducted with the aim of modelling the tissue-tool interaction force from the first step of the tissue handling skill [2, 3]. However, a mathematical model for tissue damage based on its physical property is yet to be concretized. This study aims to serve as a preliminary step to measure the fracture characteristic in biological tissues to then examine if an existing fracture model can be applied on these tissues.

In this paper, we hypothesize that biological tissues and polymeric materials share the same tearing mechanism. This is because biological tissues and polymeric materials both adopt a non-linear stress-strain relationship [4]. At a low strain, the stress-strain relationship is linear, and the slope of the stress-strain curve increases past a certain strain [4]. The elastic responses of biological tissues and polymeric materials are both dictated by the fibers that constitute them. The fibrous proteins and the polymeric fibers are also both responsible for the integrity of biological tissues and polymeric materials, respectively.

The Lake-Thomas model is a theoretical model that is widely used to estimate the tearing energy in a polymeric rubber material [5]. The tearing energy, also known as the critical tearing energy ( $T_o$ ), is the energy per unit area required to produce a new surface. The equation proposed by this model is shown in equation 1.

$$T_o = \left(\frac{3}{8}\right)^{0.5} \nu LNU \tag{1}$$

Where  $\nu$  is the number of network-strand per unit volume,  $L$  is the length of a network strand,  $N$  is the degree of polymerization, and  $U$  is the energy required to break a single monomer.

In addition to the Lake-Thomas model, Treloar proposed a statistical representation of a polymer length through the root-mean-square of a chain where the valence angles between the monomeric units follow a gaussian distribution [6]. The relationship is shown in equation 2, where  $a$  is the length of a single monomeric unit. Furthermore, based on the theory of the affine network model, the shear modulus is directly correlated to  $\nu$ , which in turn is correlated to the ratio between the polymer volume fraction ( $\phi_o$ ) and  $N$ , as shown in equation 3 [7]. Combining the theory of the affine network model (equation 3) with the statistical representation of a chain length (equation 2), the Lake-Thomas model equation can be re-written as a function of  $N$  and  $\phi_o$  as shown in equation 4.

$$L = aN^{0.5} \tag{2}$$

$$E \sim \nu \sim \frac{\phi_o}{N} \tag{3}$$

$$T_o \sim \phi_o N^{0.5} \tag{4}$$

As mentioned before, a surgeon uses the adaptive handling skill during surgery by determining the maximum applicable force (equivalent to  $T_o$  in the Lake-Thomas model), from the biological tissue’s elastic modulus ( $E$ ). In order to model this skill,  $T_o$  must be represented as a function of  $E$ . However, since  $E$  is a function of both  $\phi_o$  and  $N$ , as demonstrated by the affine network model (equation 3), different options where these two parameters can influence  $E$  must be considered. There are three manners in which  $N$  and  $\phi_o$  can influence  $E$ . The first is where  $N$  varies and  $\phi_o$  is constant. The second is where  $\phi_o$  varies while  $N$  is constant. The third is where both  $N$  and  $\phi_o$  vary simultaneously. In this paper, we decided to explore the first two options. Regarding the first option, the substitution of equation 3 into equation 4 while considering  $\phi_o$  as a constant, will result in a positive linear correlation between  $T_o$  and  $E^{-0.5}$  as shown in equation 5.1 [8-10]. As for the second option, considering  $N$  as a constant will result in a single order positive linear relationship between  $T_o$  and  $E$ , as shown in equation 5.2.

$$T_o \sim E^{-0.5} \tag{5.1}$$

$$T_o \sim E \tag{5.2}$$

In this paper, we determined  $T_o$  and  $E$  in porcine aorta, and investigated the applicability of the Lake-Thomas model onto these tissues based on equation 5.1 and 5.2. Multiple studies with the aim of validating this model through polymeric hydrogels have been conducted [8, 11]. However, to the best of our knowledge, this paper presents the first attempt at investigating the applicability of the Lake-Thomas model onto biological tissues.

## 2. Methodology

When investigating the validity of the Lake-Thomas theory through polymeric hydrogels, a dumbbell or strip shaped polymer is first prepared, and its elastic modulus ( $E$ ) is measured by the means of a tensile test. A trouser-shaped polymeric specimen with the same constitution as the dumbbell or strip-shaped specimen is then prepared, and its critical tearing energy ( $T_o$ ) is measured by another tensile test. This approach is adopted, as the mechanical property of a hydrogel can be conserved if the preparation protocol is fixed.

Due to the high variability in the mechanical properties in biological tissues, it is difficult to perform the mechanical testing on two different tissue specimens while conserving their mechanical properties. To circumvent this limitation, we decided to perform a two-step biomechanical testing on the same biological tissue to determine  $E$  and  $T_o$ . This is done by preparing a strip-shaped biological tissue specimen for the initial tensile test, and then preparing a trouser-shaped specimen from the strip-shaped specimen for the second tensile test. Using this method, we can associate a tissue-specific  $E$  with its  $T_o$ .

### 2.1 Sample Preparation (Strip-Shaped Specimens)

For this study, we harvested thoracic aorta from slaughtered pigs. The cleaning and sample preparation steps were executed 24 hours post-mortem. The thoracic aorta was first rinsed in ice-cold PBS, and then cut open in the longitudinal axis using sharp surgical scissors. The slicing was performed along the branching holes on the porcine thoracic artery. Strip-shaped specimens were then harvested using a sharp scalpel and a stencil, prepared beforehand, from the aortic sheet. The specimens were harvested in three different angles ( $0^\circ$ ,  $45^\circ$ ,  $90^\circ$ ) relative to the blood flow. The thickness of each specimen was recorded, and the tissues were preserved in ice-cold PBS before testing. The strip-shaped specimen's dimensions are shown in Fig. 1a.

### 2.2 Mechanical Testing on Strip-Shaped Specimens

Tensile tests on the strip-shaped specimens were performed with a tensile tester with a 50 N load cell (SLBL-50N, Shimadzu co. ltd, Japan) on each specimen. The extremities of the strip-shaped specimens were clamped by the tensile tester's holders, and sandpaper was set between the tissue and the holder to prevent slippage. The experimental setup is shown in Fig. 1b. The bottom arm of the tensile tester remained stationary, while the top arm pulled the specimen at a constant rate of  $50 \text{ mm min}^{-1}$ . The tensile test was terminated when the measured load reached 5 N. The biomechanical test was performed in air at room temperature, and the load and engineering strain were recorded for further analysis.

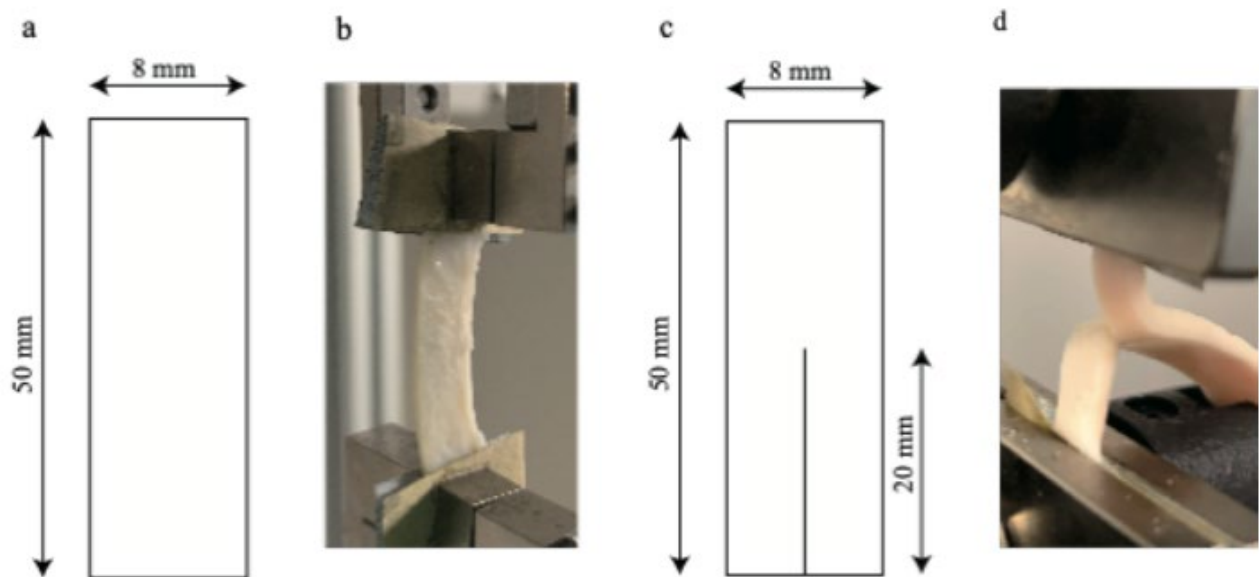


**Fig. 1 - (a) Strip-shaped specimen dimensions; (b) Experimental setup for the strip-shaped specimens; (c) Trouser-shaped specimen dimensions; (d) Experimental setup for the trouser-shaped specimens**

### 2.3 Sample Preparation (Trouser-Shaped Specimens)

Immediately after performing the mechanical testing to measure the elastic modulus, an incision onto the strip-shaped specimens was performed using a sharp scalpel and a stencil. The tissues were preserved in ice-cold PBS before testing. The trouser-shaped specimen's dimensions are shown in Fig. 1c.

### 2.4 Mechanical Testing on Trouser-Shaped Specimens

Tensile tests on the trouser-shaped specimens were performed with the same tensile tester as the one used for the strip-shaped specimens. Each leg of the trouser-shaped specimens was clamped by the holders of the tensile tester so that the legs would split apart during the experiment. Sandpaper was set between the tissue and the holder to prevent slippage. The experimental setup is shown in Fig. 1d. The bottom arm of the tensile tester remained stationary, while the top arm pulled the specimen at a constant rate of 50 mm min<sup>-1</sup>. The tensile test terminated when the trouser-shaped specimen completely ruptured into two separate pieces. The biomechanical test was performed in air at room temperature, and the load and engineering strain were recorded for further analysis.

### 2.5 Determining the Elastic Modulus ( $E$ ) and The Critical Tearing Energy ( $T_o$ )

The elastic modulus ( $E$ ) was calculated from the results of the experiments on strip-shaped specimens. The load was converted into stress ( $\sigma$ ) by dividing it by the cross-sectional area of the specimen under no load. The strain ( $\epsilon$ ) was calculated by dividing the extension by the initial specimen length. The stress-strain curve was then plotted, as shown in Fig. 2a.  $E$  was determined by the slope of the low-strain region using equation 6.

$$E = \frac{d\sigma}{d\epsilon} \quad (6)$$

The critical tearing energy ( $T_o$ ) was calculated from the results of the experiments on the trouser-shaped specimens. First, the load-strain curve for each experiment was plotted (Fig. 2b) and the point where the specimen started to tear was identified. As previously suggested by Sakai *et al.*, we took the local minimum average of the tearing force ( $F$ ) to calculate  $T_o$  in order to minimize the effect of the stick-slip behavior [6].  $T_o$  is the energy per unit area required to produce a new fracture surface. Therefore equation 7 was used to calculate  $T_o$ .

$$T_o = \frac{F \times \Delta x}{h \times \Delta x} \quad (7)$$

where  $h$  is the thickness of the trouser-shaped specimen, and  $\Delta x$  is the tearing distance.

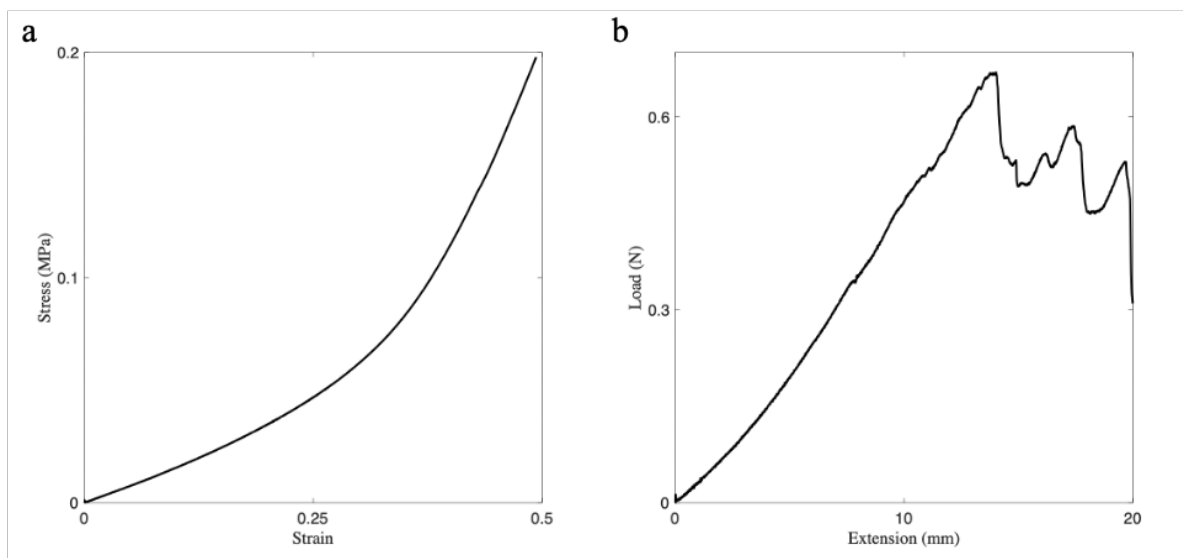


Fig. 2 - (a) Stress-strain curve from the tensile test on a strip-shaped specimen; (b) Load-extension curve from the tensile test on trouser-shaped specimens from the same sample

## 2.6 Statistical Analysis

The coefficient of determination ( $R^2$ ) was calculated by a linear regression analysis with a confidence level of 95% to analyze the linearity between  $T_o$  and  $E^{-0.5}$ , and  $T_o$  and  $E$ .

## 3. Results

In this study, we investigated the biomechanical properties of porcine thoracic aorta by performing tensile tests on strip-shaped specimens and trouser-shaped specimens. The anisotropic nature of biological tissues was addressed by harvesting the specimens from three different angles ( $0^\circ$ ,  $45^\circ$ ,  $90^\circ$ ) relative to the direction of blood flow. A particular attention was directed towards the elastic modulus ( $E$ ) and the critical tearing energy ( $T_o$ ).

### 3.1 Elastic Modulus ( $E$ ) of Porcine Thoracic Aorta

The elastic modulus ( $E$ ) is determined through the tensile test on the strip-shaped specimens. The measured values of  $E$  for each specimen angles are summarized in Table 1. We measured an average  $E$  of 0.193, 0.207 and 0.277 MPa for the specimens harvested in the  $0^\circ$ ,  $45^\circ$  and  $90^\circ$  angles relative to the blood flow, respectively.

Table 1 - Average measured  $E$  and  $T_o$  for each specimen angle

Specimen harvesting angle	$0^\circ$ (n=10)	$45^\circ$ (n=10)	$90^\circ$ (n=10)
$E$ [MPa]	$0.193 \pm 0.022$	$0.207 \pm 0.026$	$0.277 \pm 0.041$
$T_o$ [J mm <sup>-2</sup> ]	$0.454 \pm 0.184$	$0.213 \pm 0.035$	$0.418 \pm 0.212$

### 3.2 Critical Tearing Energy ( $T_o$ ) of Porcine Thoracic Aorta

The critical tearing energy ( $T_o$ ) is determined through the tensile test on the trouser-shaped specimens. The measured values of  $T_o$  for each specimen angles are summarized in Table 1. We measured an average  $T_o$  of 0.454, 0.213 and 0.418 J mm<sup>-2</sup> for the specimens harvested in the  $0^\circ$ ,  $45^\circ$  and  $90^\circ$  angles relative to the blood flow, respectively.

### 3.3 Tearing Patterns of Porcine Thoracic Aorta

Specific tearing patterns associated to the specimen harvesting angle were observed. The three different tearing patterns are illustrated in Fig. 3. The legs from the trouser-shaped specimens harvested from the  $0^\circ$  angle relative to the blood flow ruptured perpendicular to the incision on the strip-shaped specimen, while those from the  $45^\circ$  samples were separated at an angle. In the specimens from the  $90^\circ$  angle, the tear occurred down the incision on the strip-shaped specimen. A schematic representation of the trouser-shaped specimens with the collagen fiber orientation, reported by Chow *et al.*, is also shown in Fig. 3 [12].

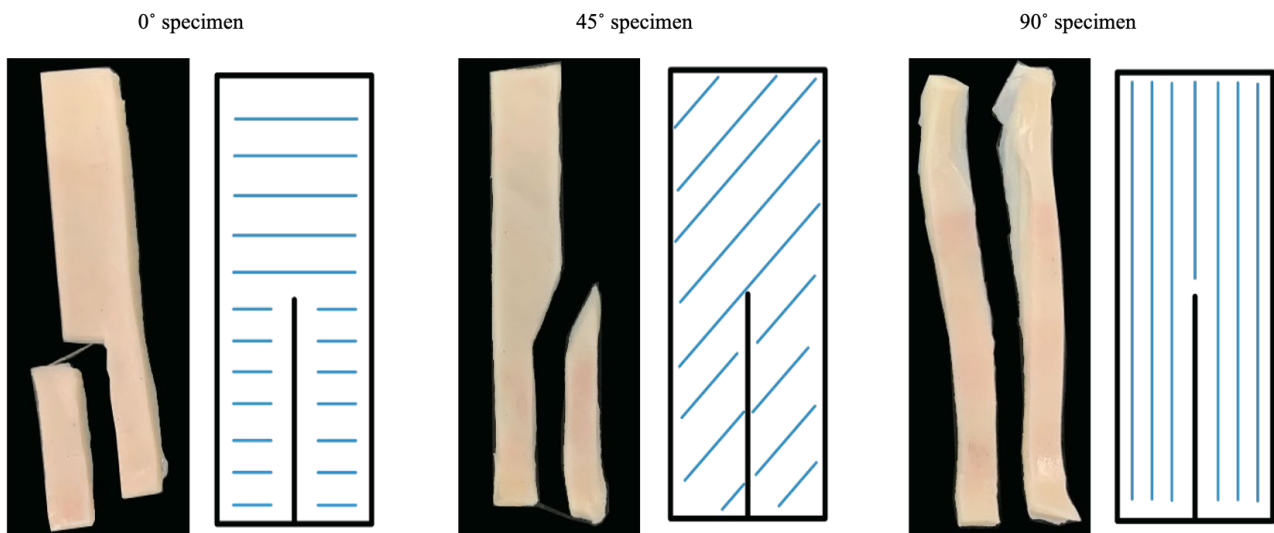
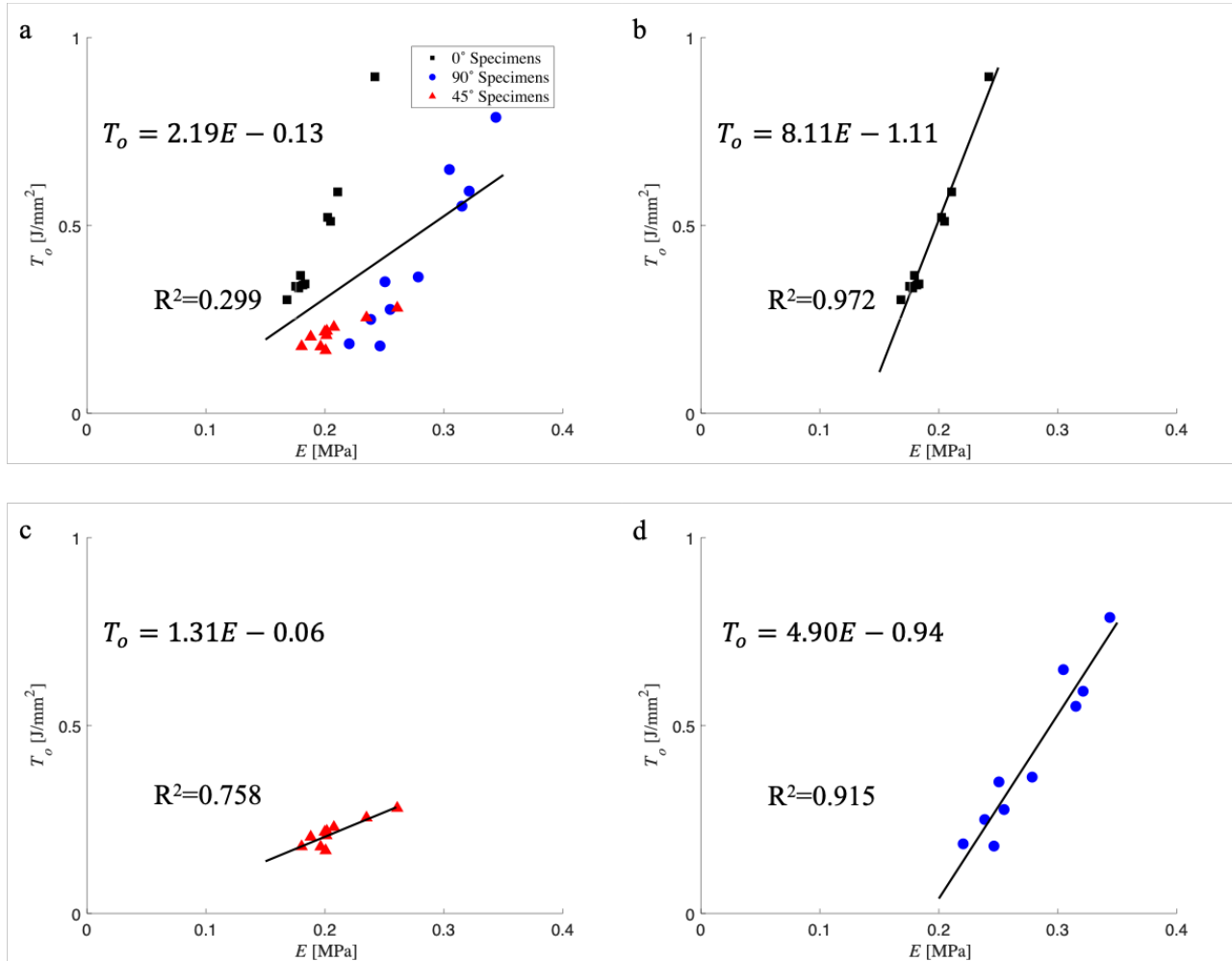


Fig. 3 - Tearing patterns for each type of specimen and collagen fiber orientation

### 3.4 Linearity between $T_o$ and $E$

Figure 4 illustrates the calculated  $T_o$  in function of  $E$ . A poor linearity was obtained, with a  $R^2$  value of 0.299 (n=30) for the overall dataset. A positive linear tendency amongst the datapoints from the identical harvesting angle can be observed. The dataset was therefore segregated based on the harvesting angles (Fig. 4b-d). The  $R^2$  value increases to 0.972 (n=10), 0.785 (n=10), 0.915 (n=10) for the specimens harvested in the  $0^\circ$ ,  $45^\circ$  and  $90^\circ$  angles relative to the blood flow, respectively. An anisotropic positive linear relationship between  $T_o$  and  $E$  can therefore be observed in porcine aorta.



**Fig. 4 - (a)  $T_o$ - $E$  relationship for each porcine thoracic aorta specimen (n=30), harvested from all three angles; (b) Dataset from specimens harvested from porcine thoracic aorta with an angle of  $0^\circ$  (n=10); (c) Dataset from specimens harvested from porcine thoracic aorta with an angle of  $45^\circ$  (n=10); (d) Dataset from specimens harvested from porcine thoracic aorta with an angle of  $90^\circ$  (n=10)**

### 3.5 Linearity Between $T_o$ and $E^{-0.5}$

The plot illustrating the calculated  $T_o$  with its associated value of  $E^{-0.5}$  is shown in Fig. 5a. The calculated  $R^2$  value for the overall dataset is 0.256 (n=30). A negative linear tendency amongst the datapoints from the identical harvesting angle can be observed. The dataset was therefore segregated based on the harvesting angles (Fig. 5b-d). The  $R^2$  values for the  $0^\circ$  specimens,  $45^\circ$  specimens and  $90^\circ$  specimens were 0.943 (n=10), 0.755 (n=10) and 0.892 (n=10), respectively. An anisotropic negative linear relationship between  $T_o$  and  $E^{-0.5}$  can therefore be observed in porcine aorta.

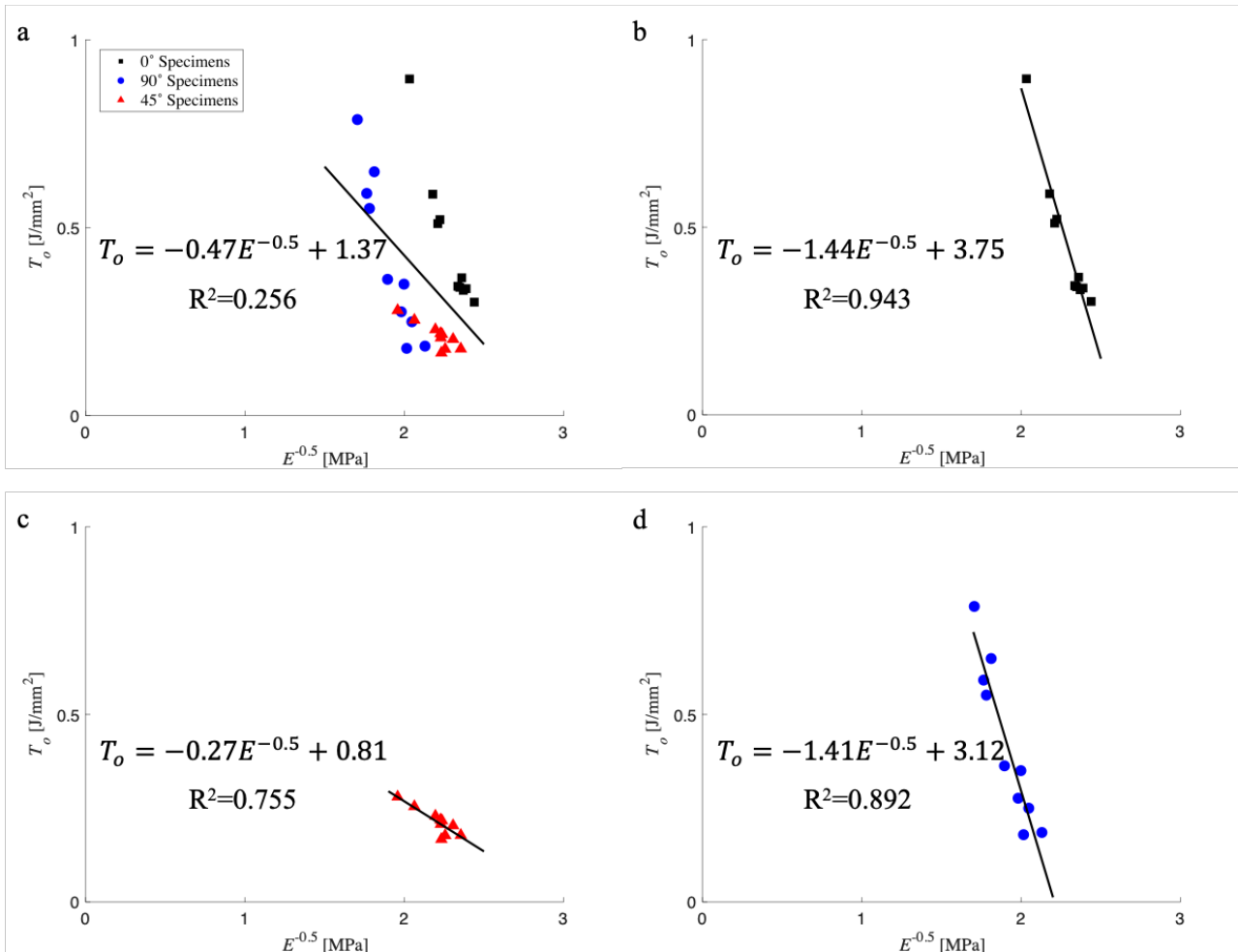


**Fig. 5 - (a)  $T_o$ - $E^{-0.5}$  relationship for each porcine thoracic aorta specimen (n=30), harvested from all three angles; (b) Dataset from specimens harvested from porcine thoracic aorta with an angle of  $0^\circ$  (n=10); (c) Dataset from specimens harvested from porcine thoracic aorta with an angle of  $45^\circ$  (n=10); (d) Dataset from specimens harvested from porcine thoracic aorta with an angle of  $90^\circ$  (n=10)**

#### 4. Discussion

In this paper, we presented two main results, based on the experiments conducted. The first main result is that there is a direct correlation between the tearing patterns on trouser-shaped porcine thoracic aorta specimens and their harvesting angles relative to the direction of blood flow. The second main result is the anisotropic positive linear relationship between  $T_o$  and  $E$  and the negative linear relationship between  $T_o$  and  $E^{-0.5}$ . Based on these two main findings, the tearing behavior of porcine thoracic aorta, the comparison between its fracture characteristic and the Lake-Thomas theory, and the anisotropic relationship between  $T_o$  and  $E$  during tissue fracture will be the subject for discussion.

##### 4.1 Tearing Behavior of Porcine Thoracic Aorta

After performing the tensile tests on the trouser-shaped specimens, we found that porcine thoracic aorta tears in a way that is highly dependent on the harvesting angle, as shown in Fig. 4. The anisotropic tearing behavior observed in this paper can be explained by the fibrous protein content in biological tissues. The two main fibrous protein constituents of a biological tissue are elastin fibers and collagen fibers. Elastin fibers dictate the elastic response of biological tissues, and collagen fibers are responsible for the integrity of the biological tissue. With a reported elastic modulus of 0.4 MPa, elastin fibers are about 250-2500 times less stiff compared to collagen fibers [4]. As shown in Table 1, the calculated  $E$  from the low strain region is in the same order as the reported  $E$  for elastin fibers. These two fibers form a network, through linkage, in the extracellular matrix of biological tissues. Chow *et al.* reported that collagen fibers have a preferential initial orientation in porcine thoracic aorta, while elastin fibers are randomly oriented [12]. They found that collagen fibers were mostly oriented in the circumferential orientation of porcine thoracic aorta.

If we overlay the initial collagen orientation on the trouser-shaped specimens (Fig. 3), we can notice that the fracture, in the trouser-shaped porcine thoracic aorta specimen, occurs parallel to the orientation of the collagen fibers. Because the mechanical property of a biological tissue is mainly influenced by the stiff collagen fibers and the elastic elastin fibers, we believe that the strain induced during the tensile test on the trouser-shaped specimens is being directed towards the elastin network that is located between the parallel collagen fibers. This elastin-collagen organization is illustrated in Fig. 5, where the fracture induced by the mechanical load occurs in the elastin network.



Fig. 5 - The elastin network between the collagen fibers break during tissue tearing

## 4.2 Comparison with the Lake-Thomas Theory

The tensile tests on the strip-shaped specimens and the trouser-shaped specimens suggested an anisotropic linear relationship between  $T_o$  and  $E$  as well as  $T_o$  and  $E^{-0.5}$ . This section of the discussion will be based on equation 3 and equation 4. More precisely, the influence of  $N$  and  $\phi_o$  on  $E$  and  $T_o$  will be the main subject for discussion. As mentioned in the introduction, based on equation 3, there are three ways where  $N$  and  $\phi_o$  can influence  $E$ . The first is where  $N$  varies and  $\phi_o$  is constant. The second is where  $\phi_o$  varies while  $N$  is constant. The third is where both  $N$  and  $\phi_o$  vary simultaneously. Regarding the first option, combining the Lake-Thomas equation (equation 4) with the affine network model (equation 3) while considering  $\phi_o$  as a constant, will result in a positive linear correlation between  $T_o$  and  $E^{-0.5}$  as the Lake-Thomas model suggests in equation 5.1. However, our results exhibited a negative correlation between these two parameters (Fig. 4 b-d), and thus possibility can be rejected.

As for the second option, substituting equation 3 into equation 4 while considering  $N$  as a constant will result in a single order positive linear relationship between  $T_o$  and  $E$  as shown in equation 5.2. Our results suggest an anisotropic positive linear relationship between  $T_o$  and  $E$  (Fig. 5 b-d). It is thus impossible to refute the possibility that the difference in the elastic modulus in biological tissues is due to a shift in the elastin fiber concentration within the specimen, and not in the structure or degree of polymerization in the elastin network. It is important to note, however, that the third option where the elastic modulus is influenced by the variation in  $N$  and  $\phi_o$  cannot be rejected. This is because although a positive linear relationship between  $T_o$  and  $E$  was reported, a more in-depth study is required to confirm the validity of the statement. Regardless of option 2 or 3,  $\phi_o$  would be the main influencing parameter in the elastic behavior in biological tissues. Further investigation regarding the effect of the elastin fiber concentration on the biological tissue's elasticity is therefore required.

A non-negligible aspect that also needs to be considered is the presence of other constituents than collagen and elastin fibers in biological tissues. In fact, biological tissues also contain a gelatinous substance called ground substance [13]. The ground substance being hydrophilic can significantly influence the hydration of the elastin and collagen fibers, which consequently will influence the mechanical property of the biological tissue in question.

## 4.3 Anisotropic Relationship Between $T_o$ and $E$ During Fracture

One of the main findings reported in this paper is the anisotropic linearity between  $T_o$  and  $E$  and  $T_o$  and  $E^{-0.5}$ . In fact, when performing the linear regression analysis on the dataset in its entirety, a low linearity was found, as shown in Fig. 4a and Fig. 5a. However, when segregating the dataset based on the harvesting angle i.e., the tensile direction, a higher linearity was verified, as shown in Fig. 4b-d and Fig. 5b-d.

We believe that the different slopes calculated during the linear regression for each type of specimen is representative of the mechanical phenomena occurring in the micro-environment around the tip of the crack. We showed that collagen fibers have an influence in the tearing patterns in porcine aorta (Fig. 3). The presence of an organized collagen fiber network oriented in the circumferential orientation of porcine aorta will cause a different stress profile around the tip of the crack. Adjusting the tensile direction into another orientation relative to the collagen fiber orientation, will therefore influence the elastin fibers that are affected by the strain induced to propagate the crack in the trouser-shaped specimens. Thus, changing the slope in the linear relationship between  $T_o$  and  $E$  and  $T_o$  and  $E^{-0.5}$ . The points discussed in the present section is subject for further investigation. For example, a microscopic observation of the area around the tip of the crack during crack propagation, where the collagen fibers and elastin fibers are visible, is required and will be conducted in future studies.



## 5. Conclusion

In robot-assisted surgery, the surgeon operates a robot to perform surgical maneuvers. One of the main limitations of robot-assisted surgery is the difficulty in transferring the surgeon's skill, such as the adaptive handling skill, onto the robot. To increase the overall safety of robot-assisted surgery, a model to estimate the maximum applicable force that can be applied onto a biological tissue without causing damage must be developed. The aim of this study is to quantitatively measure the fracture characteristic of biological tissues to investigate if the measured property matches with an existing theoretical fracture model for polymeric materials. We decided to compare the relationship between the critical tearing energy ( $T_o$ ) and the elastic modulus ( $E$ ) in biological tissues with the one for polymeric hydrogels using the Lake-Thomas model. This model has been investigated thoroughly through different types of polymeric hydrogels. However, to the best of our knowledge, this study is the first attempt to investigate the validity of this model through biological tissues. After performing a two-step tensile test on porcine thoracic aorta, we found that there was an anisotropic linear negative relationship between  $T_o$  and  $E^{-0.5}$ , and an anisotropic linear positive relationship between  $T_o$  and  $E$ . We also found that porcine thoracic aorta tears in a way that is directly correlated to the tensile direction. The nature of these results is discussed based on the conformation of collagen fibers and elastin fibers, which are the two main fibrous proteins found in biological tissues, as well as the effect of  $N$  and  $\phi_o$  on  $E$  and  $T_o$ .

While this paper suggests a correlation between  $T_o$  and  $E$  in porcine aorta, further investigation is required to build a logical mathematical model that estimates the maximum applicable force onto a biological tissue based on its elastic modulus. This model will bring an impact in the medical world, as it will significantly increase the safety of robotic-assisted surgery.

## Acknowledgement

This study was partly supported by AMED under Grand Number JP19he2302003.

## References

- [1] Panait, L., Shetty, S., Shewokis, P. and Sanchez, J. (2014). Do laparoscopic skills transfer to robotic surgery?. *Journal of Surgical Research*, 187(1), 53-58.
- [2] Sugiyama, T., Gan, L., Zareinia, K., Lama, S. and Sutherland, G. (2017). Tool-Tissue Interaction Forces in Brain Arteriovenous Malformation Surgery. *World Neurosurgery*, 102, 221-228.
- [3] Golahmadi, A., Khan, D., Mylonas, G. and Marcus, H. (2021). Tool-tissue forces in surgery: A systematic review. *Annals of Medicine and Surgery*, 65, 102268.
- [4] VanBavel, E., Siersma, P. and Spaan, J. (2003). Elasticity of passive blood vessels: a new concept. *American Journal of Physiology-Heart and Circulatory Physiology*, 285(5), H1986-H2000.
- [5] Lake, G., Thomas, A. (1967). The strength of highly elastic materials. *Proceedings of the Royal Society of London. Series A. Mathematical and Physical Sciences*, 300(1460), 108-119.
- [6] Treloar, L. (1967). *The physics of rubber elasticity*. Oxford: Clarendon Press.
- [7] Tsunoda, K., Busfield, J., Davies, C. and Thomas, A. (2000). *Journal of Materials Science*, 35(20), 5187-5198.
- [8] Sakai, T., Akagi, Y., Kondo, S., Chung, U. (2014). Experimental verification of fracture mechanism for polymer gels with controlled network structure, *Soft Matter*, 10(35), 6658-6665, 2014.
- [9] Gent, A. and Tobias, R. (1982). Threshold tear strength of elastomers. *Journal of Polymer Science: Polymer Physics Edition*, 20(11), 2051-2058.
- [10] Gent, A. (1996). Adhesion and Strength of Viscoelastic Solids. Is There a Relationship between Adhesion and Bulk Properties?†. *Langmuir*, 12(19), 4492-4496.
- [11] Akagi, Y., Sakurai, H., Gong, J., Chung, U. and Sakai, T. (2013). Fracture energy of polymer gels with controlled network structures. *The Journal of Chemical Physics*, 139(14), 144905.
- [12] Chow, M., Turcotte, R., Lin, C., Zhang, Y. (2014). Arterial Extracellular Matrix: A Mechanobiological Study of the Contributions and Interactions of Elastin and Collagen. *Biophysical Journal*, 106(12), 2684-2692.
- [13] Fung, Y. (2011). *Biomechanics*. New York: Springer.